Analysis of Unweighted Low Frequency Noise and Infrasound Measured at a Residence in the Vicinity of a Wind Farm

Kristy Hansen (1), Branko Zajamšek (1) and Colin Hansen (1)

(1) School of Mechanical Engineering, Adelaide University, Australia

ABSTRACT

To characterise the noise at several residences located nearby a South Australian wind farm, time-data files as well as the third-octave spectra have been measured indoors and outdoors using low-frequency microphones fitted with various wind shields. Five consequative nights of data have been analysed and four cases are presented here to highlight the importance of atmospheric stability and the relative wind direction between the wind farm and a residence on the measured results. In the downwind cases, two low frequency tones were detected around 28 Hz and 46 Hz and significant levels of amplitude modulation of these tones at the blade pass frequency were observed. This amplitude modulation was most prominent when atmospheric conditions were stable. The presence of these tones and the associated amplitude modulation was also observed in the vibration results, however another amplitude modulated tone at 16 Hz was found to be more significant in terms of vibration. It was also found that low-frequency indoor noise levels varied by as much as 20dB with position in a room, due to the existence of room resonances.

INTRODUCTION

A unique feature of modern wind turbines in relation to other rotating machinery is their large rotor size and low rotational speed which give rise to the generation of infrasound and low frequency noise. The generated noise can be categorised as either aeroacoustic or mechanical or both. For modern wind turbine designs, the aeroacoustic noise sources are generally dominant. However mechanical noise can become significant if there is a fault within the gearbox or generator or if the blades or tower are excited into resonant vibration and radiate noise. In this case, the character of the noise is often tonal (Moorhouse, 2007).

Each time a turbine blade passes the tower, the blade encounters flow which has been slowed down and forced to move sideways by the presence of the tower. This causes a sudden change to the angle of attack of air on the blade and the lift and drag also change abruptly (Vandenberg, 2005). The change in blade loading leads to an increase in sound pressure level at the blade-pass frequency, which is generally 0.5-1.5 Hz for modern wind turbines. Since the fluctuating loading on the blade is impulsive in nature, harmonics of the blade-pass frequency can occur and can be observable at frequencies up to 30 Hz (Vandenberg, 2005). Such high frequency harmonics are not always observed, however, and the highest order harmonic due to aerodynamic noise can be described as the last discernible peak spaced at the blade-pass frequency from the preceding peak. Tonal peaks occurring at higher frequencies are not considered to be harmonics and are thus attributed to non-aerodynamic sources.

A significant broadband contribution for frequencies less than 500 Hz is caused by inflow turbulence (Hubbard & Shepherd, 1991). Interaction between inflow turbulence and the rotating blades leads to aerodynamic loading fluctuations which cause low frequency noise generation. The amount of inflow turbulence varies with atmospheric conditions. Calculations for a modern three-bladed turbine 100m tall with 35m blade-length show that the associated peak in sound pressure level occurs at 11 Hz (Vandenberg, 2005). According to measurements, the sound pressure level caused by inflow turbulence then decreases with frequency (Hubbard & Shepherd, 1991). Close observation of figure 26 in Hubbard and Shepherd (1991) shows that there are also broadband peaks around 12 Hz, 25 Hz and 40 Hz at 1km for a MOD-1 turbine, although the source of this low frequency noise is not discussed. While this turbine is not representative of a modern design, many of the noise generation mechanisms are the same, but the relative sound levels of modern upwind turbines would be expected to be lower.

Another source of aerodynamic noise is airfoil self-noise, which is produced by the blade in an undisturbed flow (Oerlemans, 2007). It is generally higher in frequency than inflow turbulence noise and is produced by the interaction between the turbulent boundary layer on the blade and the blade trailing edge (Oerlemans, 2007).

This study focusses on the low-frequency noise contributions for reasons outlined below. Low-frequency noise is poorly absorbed by the atmosphere or ground, resulting in it being detected at much greater distances from the source than high frequency noise (Leventhall, 2003). In addition, acoustic refraction arising from atmospheric wind and temperature gradients leads to reduced attenuation of low-frequency noise in the downwind direction but little change for high frequencies (Hubbard & Shepherd, 1991). Therefore, low-frequency noise can propagate over large distances due to a combination of refraction, which causes sound waves to bend towards the ground, small atmospheric absorption and insignificant losses on reflection from the ground.

At a typical residence, noise in the mid to high frequency range is selectively attenuated by the walls and roof and the house can behave as a low-pass filter. As a consequence, the spectrum of sound inside the house is heavily weighted towards lower frequencies, which is perceived as more annoying than a well-balanced spectrum of equal loudness (Blazier

Jr., 1997). Resonances in an average-sized room are well separated at low frequencies, causing a large variation in sound pressure level as a function of location in the room (Leventhall, 2003). Control of low-frequency noise and infrasound is problematic with standard acoustic treatment.

Noise-induced structural vibration of a house is particularly perceptible in the infrasonic range or in the low-frequency range where the ear is less sensitive (Hubbard, 1982). Structural resonances occur in the range of 12-30 Hz, according to data measured for several different housing structures (Hubbard, 1982). Third-octave vibration level data from Kelley (1981) for two different housing structures that were excited by wind turbine noise showed that vibration levels were perceptible to most people according to ISO 2631-1974 (1977). It should be noted that the vibration levels associated with modern upwind rotor wind turbines would be expected to be lower than for the downwind rotor turbines discussed above. However, as will be shown, the vibration levels are still significant.

An additional characteristic of wind turbine noise is that the level can be highly variable with time, especially in stable atmospheric conditions. In these conditions, blade-tower interaction is exacerbated by the higher relative wind speed at the upper section of the rotor compared with the lower section, where the tower disturbance is most notable (Vandenberg, 2005). There is also a change in angle of attack as the blade rotates, leading to a thicker turbulent boundary layer on the blade, which causes a higher airfoil self-noise with a shift to lower frequencies (Vandenberg, 2005). This noise is amplitude modulated at the blade-pass frequency, giving rise to a signal which may contribute to a higher degree of annoyance at the residence (James, 2012). Another feature of stable atmospheric conditions is low atmospheric turbulence, resulting in different turbines rotating at a more similar speed with reduced fluctuations (Vandenberg, 2005). As a result of this near-synchronicity, there is a greater chance for blade pulses from different turbines to arrive at a particular location simultaneously, increasing the local sound pressure level at that point in time (Vandenberg, 2005).

It has been shown that the dominant source of pressure fluctuations for an outdoor microphone is the intrinsic turbulence in a flow (Morgan & Raspet, 1991). Since the wind velocity turbulence spectrum is heavily weighted to low frequencies, wind-induced noise is higher at low frequencies (Raspet *et al*., 2005). Consequently, it can be difficult to distinguish between low-frequency wind turbine noise and wind-induced noise. To address this issue, a secondary windshield can be used, which is separated from the primary windshield by a layer of air. The layer of air provides a region for viscous dissipation to reduce the turbulence generated behind the first windshield layer (Morgan & Raspet, 1991). Three different layered designs have been used in the measurements including a hemispherical, spherical and buried box windshield, as illustrated in Figures 1b – 1d.

FIELD MEASUREMENTS

Indoor and outdoor measurements were carried out for 5 days at a residence located approximately 2km south-west of the nearest turbine of a South Australian wind farm, which is made up of 37 operational turbines. The outdoor microphones were located approximately 30m from the residence in an open grass field with no bushes or shrubs. They were positioned at least 20m from the nearest trees, which were around 5-10m in height. Time series data for the outdoor microphones were acquired using a National Instruments data acquisition device at a sampling rate of 10.2 kHz for a continuous sequence of 10-minute samples. All microphones attached to this device were G.R.A.S type 40AZ with 26CG preamplifiers with a noise floor of 16dB(A) and a low-frequency linear response down to 0.5 Hz. The local wind speed and direction were measured concurrently at heights of 1.5m and 10m using a Davis Vantage Vue and a Davis Vantage Pro weather station, respectively, capable of measuring to an accuracy of 0.4m/s. The weather stations were located around 50m from the residence in an open field and are pictured in Figure 1a. The wind data were averaged over 10-minute sample periods. All third-octave and narrowband results reported in this paper refer to analysis of the entire 10-minutes of the data samples.

All four outdoor microphones were equipped with 90mm-diameter windshields as well as secondary windshields of various configurations. Two microphones were positioned at ground level, another was mounted at a height of 1.5m, and the third was located underground inside a small plywood box. The microphones located at ground level were taped horizontally at the centre of a 1m diameter aluminium plate of 3mm thickness and covered by both a primary and secondary windshield as specified in the IEC 61400-11 standard. The secondary windshield consisted of a 16mm layer of acoustic foam, covered by a layer of SoundMaster acoustic fur. The windshield was riveted to the aluminium plate and secured with a pin, with the final arrangement shown in Figure 1c. The microphone pictured in Figure 1b was mounted at a height of 1.5m using a star-dropper to minimise wind noise interference associated with the more conventional method of tripod mounting. This microphone was fitted with a secondary spherical windshield of diameter 450mm, which was attached to a steel frame, as shown in Figure 1d. The windshield materials were identical to those used for the hemispherical secondary windshield described above. The underground microphone pictured in Figure 1d was located in a 120mm x 120mm x 280mm plywood box with an acoustic foam lid, 50mm thick. The acoustic foam had a pore size of 20ppi. The top of the lid was flush with the surrounding ground to minimise the formation of eddies that would generate extraneous noise. The microphone was mounted horizontally on a custom-made shelf, which incorporated a hemispherical groove covered with a 3mm layer of rubber. The method of locating a microphone in an underground box to minimise wind noise was conceived by Betke (1996).

Figure 1. (a) Davis weather stations at 1.5m and 10m, (b) Hemispherical windshield, (c) box windshield and (d) spherical windshield.

For the indoor measurements, Brüel and Kjær (B&K) LAN-XI data acquisition hardware was used with B&K Pulse software to aquire a continuous sequence of 10-minute samples. Three microphones and two accelerometers were attached to this device. The microphones were B&K type 4955 with a noise floor of 6.5dBA and minimum frequency (ensur-

ing measurements were within 10% of flat response) of 6 Hz. One accelerometer was a B&K 4332 and the other a B&K 4335. B&K charge amplifiers type 2635 were used to amplify the signal. The three microphones were placed at various, randomly-chosen positions in the room and covered with 70mm wind shields. A microphone measurement at a single position would not have been sufficient to properly characterise the noise in the room due to the existence of standing waves, which are particularly significant at low frequencies below 200 Hz (Pedersen *et al.*, 2007). One microphone was located in the corner of the room, at the junction of 2 walls and the floor (where all room modes have anti-nodes). The instrument layout for indoors is shown in Figure 2.

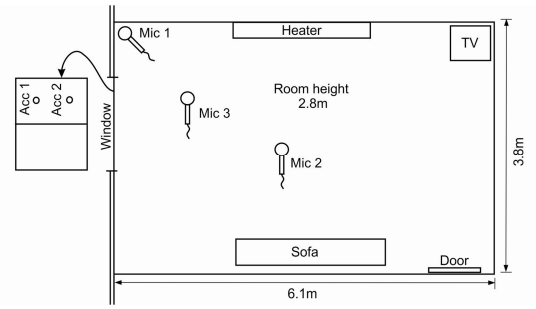

Figure 2. Schematic showing location of indoor microphones

RESULTS

To predict when wind turbine noise may have been most noticeable, an atmospheric stability plot was constructed. The value of m is determined from Equation 1, which was proposed by Kühner (1998) and used in the German Air Quality Guideline "TA-Luft" (1986).

$$m = \frac{log(v_h/v_{ref})}{log(h/h_{ref})} \quad (1)$$

This equation shows a relationship between the wind speed v_h at height h and the reference wind speed v_{ref} at a reference height h_{ref} which is governed by the atmospheric stability. Stability classes are outlined in detail in van den Berg (2004) where it was also shown that the contrast between ambient noise and wind turbine noise was greatest under stable conditions. Figure 3 shows the variation of stability with time over the 5-day measurement period. As hub-height wind speed data were unavailable, the m factor was calculated using the weather station data from 1.5m and 10m close to the microphone locations. It can be seen that conditions were the most stable on the first three nights.

A comparison between the overall unweighted, A-weighted and G-weighted sound pressure levels calculated over 10-minute intervals is shown in Figure 4 for the microphone in the hemispherical windshield. The overall unweighted level was calculated up to 200 Hz since there was negligible increase when the frequency range was increased. The overall G-weighted level was determined up to the maximum frequency for which it is specified of 315 Hz. The overall A-weighted level was calculated by applying the A-weighting filter in the time domain. The A-weighting is outlined in many regulations and standards for specifying allowable levels produced by wind farms (see for example the South Australian EPA document). The G-weighting is intended to reflect human perception of infrasonic noise (ISO-7196, 1995). Note that the measurement location was 2km from the nearest turbine in a direction ranging from WSW to SSW from the wind farm.

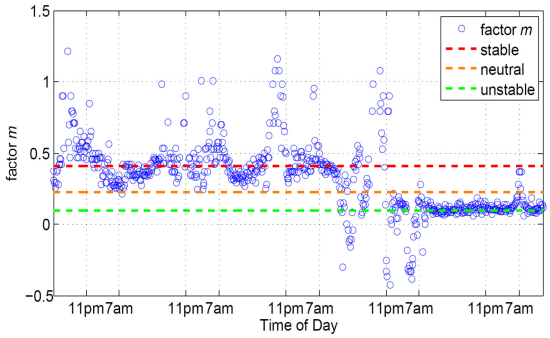

Figure 3. Degree of stability indicated by value of factor m

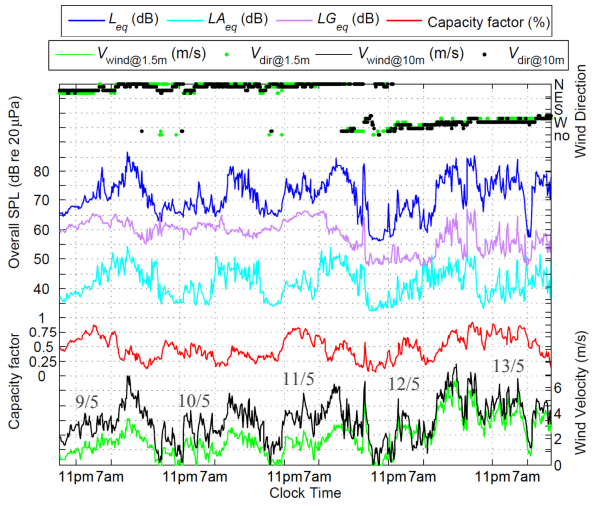

Figure 4. Comparison between the outdoor overall unweighted, A-weighted and G-weighted SPL for the measurement period. The wind speed and direction at 1.5m and 10m is also shown as well as the wind farm capacity factor.

There is a strong relationship between wind speed variations and fluctuations in the unweighted noise level, which is less significant for the A-weighted levels and much less pronounced for the G-weighted levels. It can be seen that the wind direction was predominantly NE for the first three nights of the measurement period, during which time the instruments were downwind from the wind farm. The wind farm capacity factor for the five different nights is also shown and the wind farm is clearly operating at night for the entire measurement period.

In order to find the contribution of various frequency bands to the overall unweighted noise level, third-octave spectra were plotted for the four outdoor microphones with different windshield configurations. Four cases of interest were selected, which corresponded to a relatively high power output with two different wind directions[1-2], the most stable downwind conditions[3] and a relatively low power output[4] over the measurement period. These cases are typical for a number of 10-minute average samples which were acquired under similar conditions during the measurement period. Note that wind speed and direction were measured at microphone height. The conditions associated with these measurement times are summarised in Table 1. The results are shown in Figure 5, where it can be seen that measured levels are generally at

least 10dB above the microphone noise floor, which was measured in the anechoic chamber at the University of Adelaide. However, for some measurements, the sound levels at infrasonic frequencies are close to the microphone noise floor and these results should be viewed with caution. Noise floor results for the 16 Hz and 20 Hz third-octave bands have not been included as there is a problem in the anechoic chamber for these frequencies.

Table 1. Summary of wind conditions and wind farm capacity factor for selected measurement times

Case	Date/Time	Wind speed (m/s)	Wind Direction	Capacity factor	Stability factor
High power downwind[1]	9/5, 3:32	0.9	NE	86%	0.42
High power upwind[2]	13/5, 5:02	4.5	WSW	84%	0.11
Stable downwind[3]	9/5, 12:02	0.4	ENE	61%	0.85
Low power[4]	12/5, 12:02	0.4	NW	16%	0.90

Figure 6 shows that there is a spectral peak in the 50 Hz third-octave band for the "high power downwind" and "stable downwind" cases and this could easily be mistaken for electrical noise. This peak appears consistently in 10-minute average results for a number of hours. However, this peak is not present in the results for the "high power upwind" and the "low power" cases, which confirms that the noise source is not related to the measurement system. In both cases where the 50 Hz peak was identified, the atmospheric conditions were stable, the residence was in the downwind direction from the wind farm and the wind farm was operating at over 50% capacity. Noise in the 50 Hz third-octave band would be audible to a person with normal hearing according to international standard ISO 389-7 (2005), which specifies the threshold of hearing for free-field tonal noise. Other less noticeable peaks in the spectra can be seen in the low infrasonic frequency range for the "stable downwind" case.

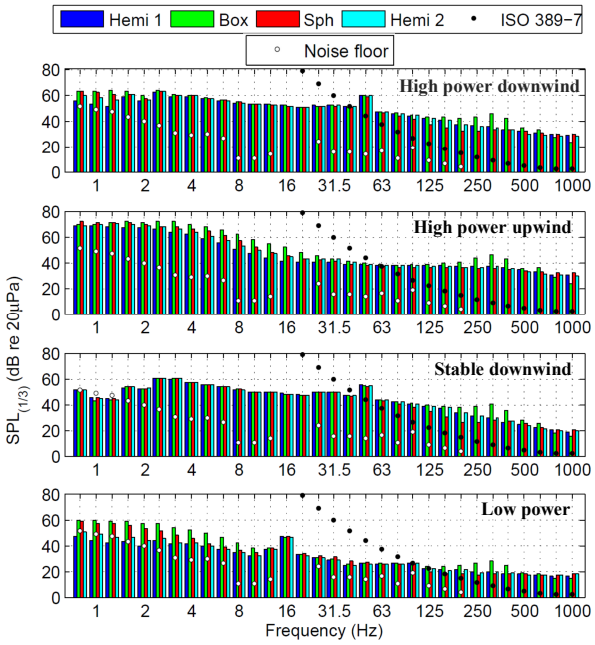

Figure 5. Third-octave spectrum plots for times and conditions listed in Table 1 showing results for microphones with a hemispherical, box and spherical windshield, the ISO 389-7 hearing threshold curve and the microphone noise floor.

These results indicate that the hemispherical windshields were least affected by wind-induced noise compared to the other windshield configurations, as these microphones measured the lowest infrasonic sound pressure levels. However, a more detailed analysis of the wind-induced noise component for each wind-shield is required to verify this result. It is also evident that there can be significant differences in the measured noise levels for microphones in the buried box and spherical windshields in comparison with microphones in the hemispherical windshields. This is particularly evident at very low frequencies and for frequencies greater than 100 Hz. Even though the microphones in the hemispherical windshields were placed 18m apart, the results are almost identical. This indicates that the relative performance of the different windshields needs further investigation for these frequencies and this will be the subject of future work.

The third-octave spectra plots for simultaneous indoor measurements are shown in Figure 6. Results are plotted for three microphones placed at various positions around the room, where "mic 1" was located in the room corner. For all third-octave bands, the measurements are at least 20dB above the microphone noise floor. For most infrasonic frequencies, there is negligible difference in the sound pressure levels measured at different positions around the room. This indicates that a single microphone would have been sufficient to measure at these frequencies. On the other hand, for the 16 Hz third-octave band, measured values begin to diverge, which can be attributed to structural resonances and room resonances. Resonance effects are most notable for the 25 Hz and 31.5 Hz third-octave bands, where the sound pressure levels measured by two of the microphones are at least 20dB higher than the other microphone. This is consistent with the fact that the longest dimension of the room was 6.2m, which would have an associated resonance frequency around 28 Hz. In addition, the measured sound pressure levels indoors are higher than those measured outdoors for these two octave bands. Since the residence was unoccupied, internal noise sources are considered to be negligible and hence it can be assumed that the noise in these third-octave bands originated outdoors.

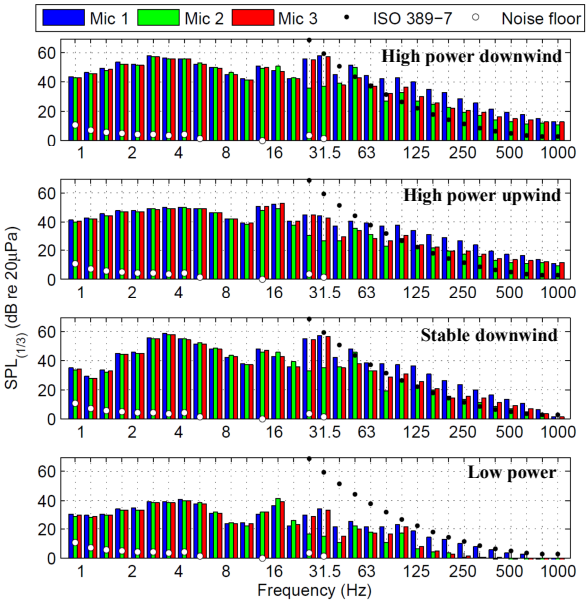

Figure 6. Third-octave spectrum plots for times and conditions listed in Table 1 showing results for indoor microphones, the ISO 389-7 hearing threshold curve and the microphone noise floor.

It can be seen that internal noise levels at 20 Hz are at least 30 dB below the audibility threshold for a person with normal hearing according to international standard ISO 389-7 (2005). Hence, these measurements indicate that infrasound is not likely to be a potential issue in terms of audibility. However, noise levels at frequencies of 50 Hz and above are clearly audible in some cases.

In the frequency range 63 Hz ≤ f ≤ 800 Hz, the corner microphone measured the highest sound pressure level since it was positioned at the antinode for all room resonances, whereas other microphones were at varying locations with respect to antinodes. When there are many modes, the corner measurement is highest due to it being the anti-nodal location for all room resonant modes.

The difference between outdoor and indoor third-octave sound pressure levels is shown in Figure 7. This difference was calculated between a microphone with the hemispherical windshield and all three indoor microphones. The intention is to portray the variation in sound pressure level for different positions in a room.

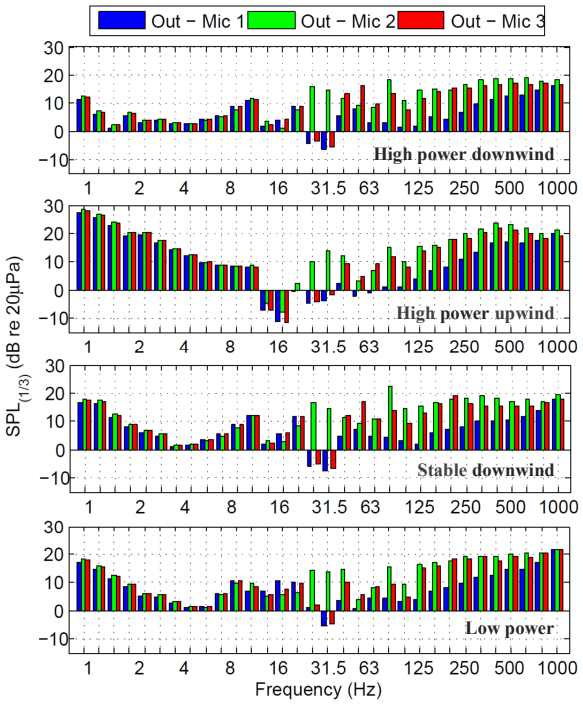

Figure 7. Third-octave spectrum plots for times and conditions listed in Table 1 showing results for the difference between levels measured outdoors (with hemispherical windshield) and indoors.

It is believed that the large difference in sound pressure level at low infrasonic frequencies is due to the interaction between atmospheric turbulence and the outdoor microphone. It appears that the secondary windshield is not very effective at such low frequencies. For the majority of infrasonic frequencies there is only a small attenuation provided by the house. For the 25 Hz and 31.5 Hz third-octave bands, a room resonance can be identified by an increased sound pressure level in some room locations and a decreased level in another room location. The variation in sound pressure level within the room also occurs for the third-octave bands from 40-100 Hz, but to a lesser extent. This frequency range contains resonances at 45 Hz and 62 Hz corresponding to the room dimensions of 3.8m and 2.8m, respectively. However, these resonances exhibit higher damping, resulting in a reduced sound pressure level variation with position in the room. At 125 Hz and above, the outdoor-to-indoor sound pressure level difference is consistently above 10dB, except for the corner microphone. An anomaly can be observed in the results for the "high power upwind" case where the indoor level in the 12.5 Hz and 16 Hz third-octave bands is higher. It is possible that there is a structural resonance in this frequency range which is excited by wind turbine noise or atmospheric turbulence. It will be shown later in the paper that the excitation source is most likely wind turbine noise.

To ascertain more detailed information about the spectral content of both the outdoor and indoor signals, a narrowband analysis was carried out with a frequency resolution of 0.1 Hz. The narrowband plots have been divided into two frequency ranges to improve resolution. The outdoor results are shown in Figures 8(a-d) and the corresponding cases for the indoor measurements are shown in the adjacent column in Figures 9(a-d). The narrowband analysis reveals many important details that can be overlooked through focussing solely on third-octave band levels. The most crucial advantage of viewing the narrowband spectra is that amplitude modulation of a spectral peak can be identified. Amplitude modulation is characterised by sidebands adjacent to the spectral peaks, which have spacing equal to the blade-pass frequency. A narrowband analysis can also show the presence of the blade-pass frequency and its harmonics.

For the outdoor results, amplitude modulation is most significant in the "stable downwind" case shown in Figure 8(c), where the atmosphere was stable, the residence was downwind from the wind turbines and the wind farm was operating at 61% capacity. The wind at the residence was also light during this measurement which would have minimised the wind-induced noise on the microphone. The lowest peak frequency of 0.8 Hz and its harmonics are clearly visible in the upper section of Figure 8(c). This frequency peak of 0.8 Hz corresponds to the blade-pass frequency of 0.8 Hz at the nominal rotational speed of 16.1rpm for a Vesta V90-3 MW wind turbine (Vestas Wind Systems, n.d.). The other peaks are spaced at 0.8 Hz up to a frequency of 7.2 Hz and are thus clearly the harmonics of the blade-pass frequency. Tonal peaks are also measured at 28 Hz and 46.7 Hz, however these are not considered to be harmonics of the blade-pass frequency. The presence of side-bands spaced at 0.8 Hz for these tonal peaks indicates that they are amplitude modulated at the blade-pass frequency and this suggests that the noise originates from the turbines. The tonal characteristic implies that the noise could be associated with an aeroelastic phenomenon associated with the tower and blades or that there is a problem with the drive system. Ambrose and Rand (2011) also observed amplitude modulation of tonal noise at low frequencies. They measured the tonal frequency of 22.9 Hz with an amplitude modulation frequency of 0.7 Hz in the vicinity of a "NOTUS" wind turbine. The tone was considered as a "signature of the wind turbine's acoustic profile" (Ambrose and Rand (2011).

For the "high power downwind" and "low power" cases, shown in Figure 8(a) & (d), it is possible to identify tonal noise; however amplitude modulation is not clearly evident. On the other hand, the blade-pass frequency and its harmonics are present in both figures. In the former case, peaks occur at 28.1 Hz and 46.8 Hz; however, they are broadband in nature, which suggests that amplitude modulation may still

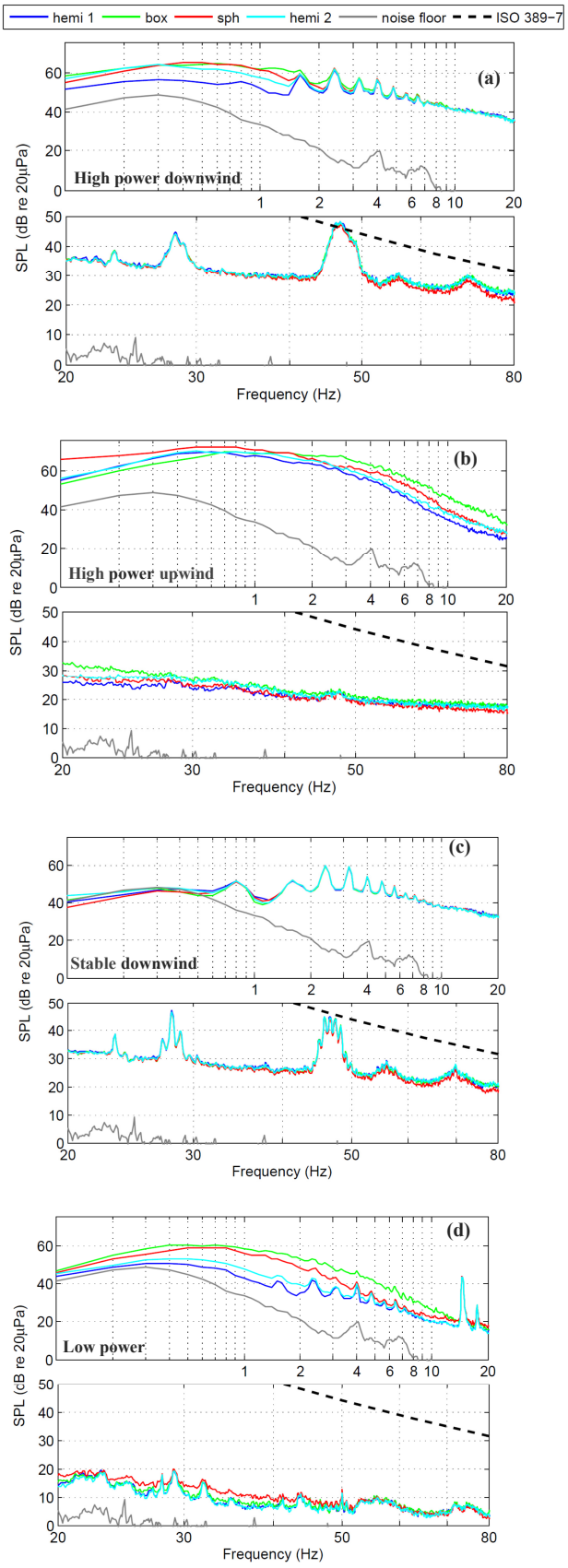

Figure 8. Narrowband plots for the Table 1 cases showing results for outdoor microphones with a hemispherical, box and spherical windshield, the ISO 389-7 hearing threshold curve and the microphone noise floor.

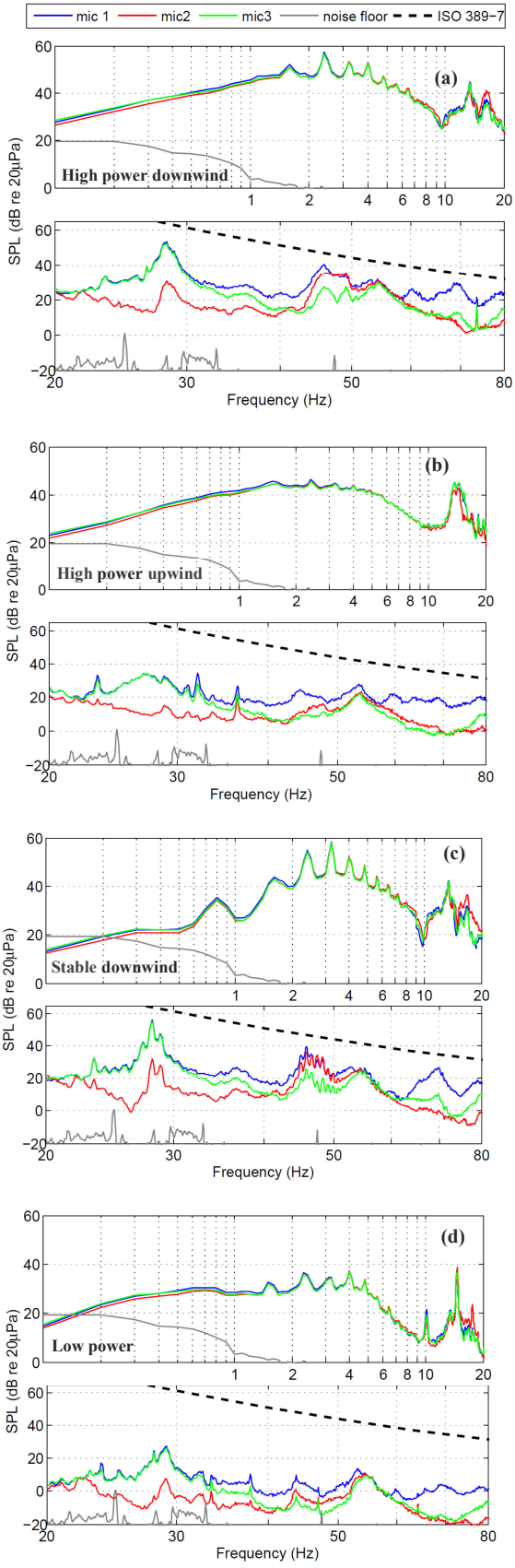

Figure 9. Narrowband spectra for the cases described in Table 1 showing results for indoor microphones positioned as shown in Figure 2, the ISO 389-7 hearing threshold curve and the microphone noise floor.

be occurring but the wind turbine rotor speed may be varying slightly, causing the peaks to broaden. In the latter case, there are narrower peaks at 14.6 Hz and 29 Hz but they are relatively small. This is consistent with the relatively low capacity factor for the wind farm for this case (16%).

The "low power" case shown in Figure 8(d) is the only measurement for which the blade-pass frequency and its harmonics are not visible in the narrowband plot. While this could be attributed to the general increase in infrasound associated with the higher wind speed, it should also be recalled that this is the only case that the residence was directly upwind of the wind farm and that the atmospheric stability was close to neutral. In addition, the spectra from 20 Hz to 80 Hz show a complete absence of tones and the sound pressure level in this frequency range is lower than the baseline level (ignoring the tones) of the "stable downwind" case.

According to ISO 389-7 (2005), the measured outdoor noise in the frequency range of 0 - 80 Hz is lower than the perception level of single frequency tones for most people, except for the "high power downwind" case in the frequency range between 46 Hz and 47.5 Hz for a person with normal hearing.

For the indoor results shown in Figure 9(a-d), the data presented below 6 Hz is uncalibrated and hence does not reflect the true sound pressure level for these frequencies. However, peaks at the blade-pass frequency and harmonics indicate that the microphones are still capable of measuring (albeit with decreased accuracy) below 6 Hz.

Consistent with the outdoor results, the most notable amplitude modulation occurred for 28 Hz and 46.7 Hz in the "stable downwind" case shown in Figure 9(c). The blade-pass frequency and its harmonics can also be identified in the upper section of this figure. The relative amount of amplitude modulation for the three microphones is similar; however there is a large variation in the sound pressure level peaks with room position. The highest sound pressure levels are measured by the microphone placed in the corner, which is expected as this corresponds to an anti-nodal position for all room modes.

Results for all four cases share some similarities, which include an increase in the peak sound pressure level around 28 Hz and a decrease around 46 Hz from outdoors to indoors. Also, there exists low frequency peaks at 14 Hz and 16 Hz in Figure 9(a-d), which are amplitude modulated at the blade-pass frequency. This is evidenced by the side-bands which are spaced at an integer multiple of the blade-pass frequency. These peaks are not necessarily evident in the outdoor spectra and this highlights the importance of simultaneous outdoor and indoor measurements. Such peaks can be seen to consistently occur for the indoor measurements shown in Figure 9(a-d), but they are only visible in Figure 8(d) for the outdoor measurements. The presence of amplitude modulation at the blade-pass frequency implies that the noise originates at the wind farm.

The corner microphone consistently measured higher sound pressure levels than the other microphones for all four cases, as expected. All indoor results in the frequency range of 0.5 – 80 Hz showed that the noise was below the perception level of most people for single frequency tones according to ISO 389-7 (2005).

Third-octave vibration spectra, measured with window-mounted accelerometers, are shown in Figure 10 together with the instrumentation noise floor measured on a 50 mm thick foam blanket placed on the floor of the anechoic chamber at University of Adelaide. For this case, all data points for the noise floor have been included, since the frequency range containing the problem frequencies in the anechoic chamber is also of interest in the measurements. Referring to Figure 10, it is evident that the most significant contribution to vibration occurs in the 16 Hz third-octave band, which could correspond to a structural resonance of the wall or window of the house. The measured level is close to the limit of acceptability for building vibration specified in AS2670.2 (1990). Other relatively high vibration levels are evident in the third-octave bands from 12.5 Hz to 63 Hz but these are below the limits specified in AS2670.2 (1990). The highest levels in this frequency range for the four measurements correspond to the "high power downwind" and the "stable downwind" cases, for which the sound pressure level was also highest. Variation in the vibration levels measured with the different accelerometers is attributed to their different locations on the window.

In the "high power upwind" case, the relatively higher infrasonic acceleration levels could be a result of increased atmospheric turbulence associated with the higher wind speed for this case. The relatively higher infrasonic acceleration measured in the "low power" case (compared to the "high power upwind" and "stable downwind" cases) may be related to the NW wind blowing over the house and generating turbulence on the lee side of the house.

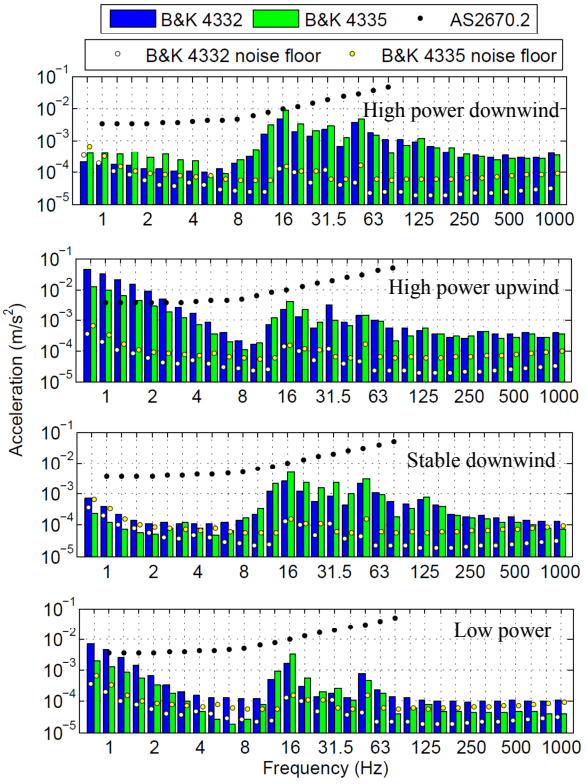

Figure 10. Third-octave vibration acceleration spectrum measured with two accelerometers located at different positions on the same window. AS2670.2 acceleration base curve for building vibration combined direction is also shown.

The narrowband vibration results obtained using a frequency resolution of 0.1 Hz show that the frequencies of the spectral peaks are similar to those identified in the acoustic analysis. This implies that the vibration is caused by noise-induced structural vibration. There is also evidence of amplitude modulation, particularly around 47 Hz, which is indicated by the side-bands that are spaced at an integer multiple of the blade-pass frequency. Amplitude modulation also occurs around 16 Hz but the side-band peaks are less distinct. Hence it can be deduced that the vibration measured in the 16 Hz third-octave band shown in Figure 10 is caused by noise that originates at the wind farm. It is likely that one or more frequencies in this third octave band excite structural resonances which lead to vibration levels that exceed the limits for building vibration recommended in AS2670.2 (1990).

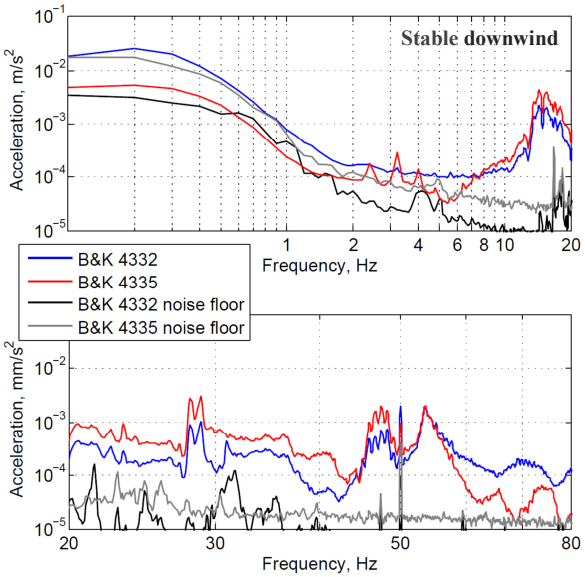

Figure 11. Narrowband plot of "stable downwind" case in Table 1 showing indoor vibration acceleration results measured with two accelerometers located at different positions on the same window. Accelerometer noise floors are also shown.

Amplitude modulation of noise

Further evidence pertaining to the existence of amplitude modulation of the noise at the measurement locations was obtained through use of the Hilbert transform. The "stable downwind" case was selected for analysis since the most noticeable amplitude modulation was indicated for this measurement. The signal was band-pass filtered between 45 Hz and 50 Hz using a third-order Butterworth filter to focus on the tone at 46.7 Hz. The Hilbert transform was used to find the envelope of the filtered signal as shown in Figure 12.

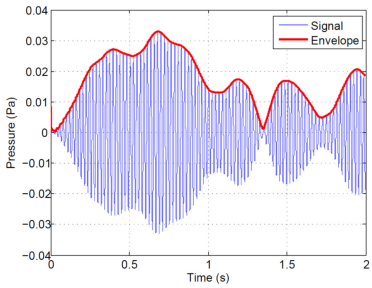

Figure 12. Signal envelope obtained using Hilbert transform plotted with signal. Outdoor signal of the "stable downwind" case was band-pass filtered between 45 and 50 Hz.

The envelope signal was then analysed for frequency content and the resulting peaks showed the amplitude modulation frequencies. In this analysis, the absolute value of the Hilbert transform was calculated, the mean value was subtracted and the result was squared. A narrowband analysis with a resolution of 0.1 Hz was then carried out on the resulting signal. Following this procedure led to the clearest representation of the amplitude modulating frequencies. Figure 13 shows that the blade-pass frequency at 0.8 Hz and the first two harmonics contribute most noticeably to amplitude modulation.

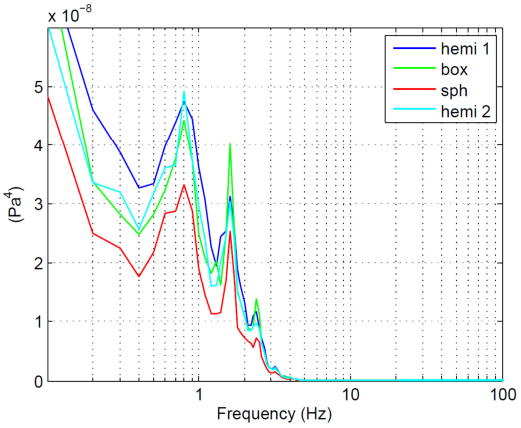

Figure 13. Squared envelope spectrum of outdoor signal corresponding to the "stable downwind" case. Signal was band-pass filtered between 45 and 50 Hz and spectral frequency resolution is 0.1 Hz.

To provide a better visual representation of the amplitude modulation that occurred for the "stable downwind" case in the frequency range of 45 Hz to 50 Hz, a sonogram is shown in Figure 14. The signal was band-pass filtered between 45 Hz and 50 Hz using a third-order Butterworth filter and then analysed with a frequency resolution of 5 Hz. This frequency resolution corresponds to an averaging time of 0.2s. For the 30 second interval shown in Figure 14, the maximum variation in rms sound pressure level is from 35dB to 60dB. However, the amplitude of the fluctuations in sound pressure level vary significantly from one measurement period to the next. The time interval between the peaks in Figure 14 corresponds not only to the blade-pass frequency but also to its harmonics.

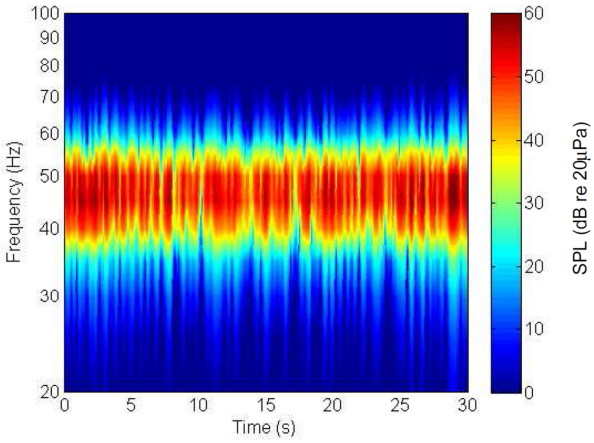

Figure 14. Sonogram with frequency resolution of 5 Hz showing amplitude modulation associated with the the "stable downwind" case measurement which has been band-pass filtered between 45 Hz and 50 Hz.

CONCLUSIONS

Several spectral characteristics have been identified in this study which may be overlooked in an analysis that considered time-averaged third-octave levels exclusively. The existence of two tones around 28 Hz and 46 Hz that have corresponding rms sound pressure levels close to the threshold of audibility (for most people) for single frequency tones, has been established. It has also been shown that these tones are amplitude modulated at approximately 0.8 Hz, which corresponds to the blade-pass frequency. The 15 dB of amplitude modulation makes this noise much more noticeable and annoying than would be the case for the steady tonal sound used to establish the thresholds of audibility. Peaks at the blade-pass frequency and its harmonics have also been measured.

Vibration results indicate that acceleration levels measured in the 16 Hz third-octave band are close to the recommended upper limit for building vibrations in AS 2670.2 (1990). The presence of amplitude modulation at this frequency in the narrowband results suggests that the housing structure is excited by noise that originates at the wind farm.

Analysis of four representative cases based on times where the wind farm power output, wind speed, wind direction and stability were different has shown that the measured sound pressure level and degree of amplitude modulation is highly dependent on these variables. The worst case conditions for the tonal peaks corresponded to the cases where the residence was located downwind from the wind farm. In terms of amplitude modulation, the worst case occurred in stable, downwind conditions where the wind farm was operating at a capacity greater than 50%. These characteristics were observed for a number of 10-minute averages for a given condition but all results are not presented in this paper due to space restrictions. The nature of the observations suggests that there is a possible aeroelastic phenomenon associated with the tower and blades or a problem with the wind turbine drive system.

It has also been shown that low-frequency indoor noise levels are highly variable with room postion and could differ by as much as 20dB from one position to another. This occurred at frequencies in the range where room resonances would be expected to exist. A possible structural resonance was identified at 16 Hz, where the vibration levels were relatively higher. The sound pressure level at this frequency was also found to increase indoors relative to outdoors for one of the measurement cases.

For the different windshield configurations, there is good agreement in the measurements of the blade-pass frequency, tonal noise and amplitude modulation. However, there are some discrepancies in the infrasonic range for the broadband noise component, which is due to differences in the secondary windshield geometry and location. This would affect the strength of turbulence incident on the microphones.

ACKNOWLEDGEMENTS

Support from the Australian Research Council is gratefully acklowledged. We are also very thankful to all of the residents who allowed us to use their premises, especially for the indoor measurements. Thanks to Andrew and Paul Miskelly for supplying wind farm power output data and for the excellent weather reports available from “Weatherzone.”

REFERENCES

Ambrose, SE and Rand, RW 2011, *The Bruce McPherson infrasound and low frequency noise study*; *adverse health effects produced by large industrial wind turbines confirmed*. December 14, 2011.

Blazier, WE 1997, *RC Mark II: A refined procedure for rating noise of heating ventilating and air conditioning (HVAC) systems in buildings*, Noise Control Engineering, vol. 45, pp. 243-250.

Hubbard, HH 1982, *Noise-induced house vibrations and human perception*, Noise Control Engineering, vol. 19, no. 2, pp. 49-55.

Hubbard, HH and Shepherd KP 1991, *Aeroacoustics of Large Wind Turbines*, Journal of Acoustical Society of America vol. 89, no.6, pp. 2495-2508.

International Organization for Standardization 1995, *Acoustics – Frequency weighting characteristic for infrasound measurements*, ISO 7196, Geneva.

International Organization for Standardization 2005, *Reference threshold of hearing under free-field and diffuse-field listening conditions*, ISO 389-7, Geneva.

James, RR 2012, *Wind turbine infra and low frequency sound: warning signs that were not heard*, Bulletin of Science, Technology and Society, vol. 32, no. 2, pp. 108-127.

Kelley, ND, McKenna, HE, Hemphill, RR, Etter, CL, Gatfelts, RL and Linn, NC 1985, Acoustic noise associate with the MOD-1wind turbine: its source, impact and control, SERI TR-635-1166.

Kühner, D 1998, *Excess attenuation due to meteorological influences and ground impedance*, Acustica - Acta Acustica 84, 870–883.

Leventhall, G, Pelmear, P and Benton, S, *A review of published research on low frequency noise and its effects*, Defra Publications, London.

Moorhouse, A, Hayes, M, von Hünerbein, S, Piper, B and Adams, M 2007, *Research into Aerodynamic Modulation of Wind Turbine Noise: Final report*, University of Salford, Manchester.

Morgan, S and Raspet, R 1991, *Investigation of the mechanisms of low-frequency wind noise generation outdoors*, Journal of Acoustical Society of America, vol. 92, no. 20, pp. 1180-83.

Oerlemans, S, Sijtsma, P and Mendez-Lopez, B 2007, Location and quantification of noise sources on a wind turbine, Journal of Sound and Vibration, vol. 299, pp. 869-883.

Pedersen, S, Moller, H and Persson Waye, K 2007, *Indoor measurements of noise at low frequencies – problems and solutions*, Journal of Low Frequency Noise, Vibration, and Active Control, vol. 26, no. 4, pp. 249-270.

Raspet, R, Webster, J and Dillon, K 2005 *Framework for wind noise studies*, Journal of Acoustical Society of America, vol. 119, no. 2, pp. 834-843.

Standards Australia Committee on Vibration and Shock-Human Effects 1990, *Evaluation of human exposure to whole-body vibration*, AS 2670.2, Standards Australia, Homebush NSW.

TA-Luft 1986, *Erste Allgemeine Verwaltungsvorschrift zum Bundes-Immissionsschutzgesetz* - Technische Anleitung zur Reinhaltung der Luft (*First general directive to the federal immission protection act* - Technical guideline for clean air), (in German).

van den Berg, GP 2004, *Effects of wind profile at night on wind turbine sound*, Journal of Sound and Vibration vol. 277, pp. 955-970.

van den Berg, GP 2005, *The beat is getting stronger: The effect of atmospheric stability on low frequency modulated sound of wind turbines*, Journal of Low Frequency Noise, Vibration, and Active Control, vol. 24, no. 1, pp. 1-24.

Vestas product brochure, n.d., Viewed 17 August 2013, <http://www.ceoe.udel.edu/windpower/docs/ProductbrochureV90_3_0_UK.pdf>